Translating Numerical Concepts for PDEs into Neural Architectures[*]

Tobias Alt, Pascal Peter, Joachim Weickert, and Karl Schrader

Mathematical Image Analysis Group, Faculty of Mathematics and Computer Science,
Campus E1.7, Saarland University, 66041 Saarbrücken, Germany.
{alt, peter, weickert, schrader}@mia.uni-saarland.de

Abstract. We investigate what can be learned from translating numerical algorithms into neural networks. On the numerical side, we consider explicit, accelerated explicit, and implicit schemes for a general higher order nonlinear diffusion equation in 1D, as well as linear multigrid methods. On the neural network side, we identify corresponding concepts in terms of residual networks (ResNets), recurrent networks, and U-nets. These connections guarantee Euclidean stability of specific ResNets with a transposed convolution layer structure in each block. We present three numerical justifications for skip connections: as time discretisations in explicit schemes, as extrapolation mechanisms for accelerating those methods, and as recurrent connections in fixed point solvers for implicit schemes. Last but not least, we also motivate uncommon design choices such as nonmonotone activation functions. Our findings give a numerical perspective on the success of modern neural network architectures, and they provide design criteria for stable networks.

Keywords: numerical algorithms · partial differential equations · convolutional neural networks · nonlinear diffusion · stability

1 Introduction

The remarkable success of convolutional neural networks (CNNs) has triggered many researchers to analyse their behaviour and to come up with mathematical foundations and stability guarantees. One strategy consists of interpreting networks as approximations of evolution equations; see e.g. [3,22,23]. Then training a network comes down to parameter identification of ordinary or partial differential equations (PDEs). This can be challenging, since it requires various model assumptions: Without additional smoothness assumptions, the models may become very complicated involving millions of parameters. Moreover, connecting a discrete network to a continuous evolution equation involves ambiguous limit assumptions: The same discrete model can approximate multiple evolution equations with different orders of consistency.

We address these problems by following two guiding principles:

1. We refrain from the *analytic* strategy of translating a complex neural network into a compact model, since it involves the discussed problems and only analyses how a network is, but not how it should be. Instead we pursue a *synthetic* approach: We translate successful concepts into networks. This is easier, and it allows to understand how a network should be to guarantee desirable qualities such as stability and efficiency.
2. Our concepts of choice are numerical algorithms rather than continuous models. This avoids ambiguities in the limit assumptions. Similar to neural architectures, numerical algorithms can be applied to a multitude of models. We believe that the design principles of modern neural networks realise a small but powerful set of numerical strategies as a basis of their success.

Thus, we want to justify key components of neural architectures and derive novel design principles by translating popular numerical algorithms into networks.

Our Contributions. As an exemplary starting point and a basis for exploring different numerical algorithms, we consider a general evolution equation for higher order nonlinear diffusion in 1D.

First we show that an explicit finite difference discretisation can be interpreted as a residual network (ResNet) [11]. This gives two central insights: The diffusion flux function determines the activation function of the ResNet, and the two convolutional filters follow a transposed structure. This motivates the use of nonmonotone activation functions and allows us to guarantee stability in the Euclidean norm for specific ResNets. Moreover, we identify the skip connections in the ResNet as discrete time derivatives.

Additional interpretations of skip connections are obtained with alternative numerical methods based on fast semi-iterative (FSI) accelerations of explicit schemes [9] and on fixed point algorithms for fully implicit schemes. We show that the latter ones can be regarded as recurrent neural networks [12].

Since multigrid methods [2] are efficient numerical methods for PDEs, it is worthwhile to analyse them as well. We demonstrate that they have structural connections to U-nets [20], shedding some light on their efficiency.

Our results do not only inspire general design criteria for neural networks as well as stable architectures. They also provide structural insights into ResNets, RNNs and U-nets from the perspective of numerical algorithms.

Related Work. Our philosophy to translate numerics into neural networks is shared in [14,18]. Both works motivate additional skip connections in ResNets from multistep schemes for ordinary differential equations. Our paper provides alternative motivations via time discretisations, acceleration via extrapolation, as well as fixed point schemes for implicit discretisations.

The stability of ResNets is studied from a differential equations perspective in [21,22,27]. Particularly, Ruthotto and Haber [22] show stability in the Euclidean norm for a specific form of residual networks. However, they require the

activation function to be monotone. In contrast to their approach, our theory allows nonmonotone activation functions.

Several works connect multigrid ideas and CNNs, e.g. to learn the restriction and prolongation operators [8], or to couple feature channels for parameter reduction [6]. He and Xu [10] present a CNN architecture implementing multigrid approaches, however without connecting it to a U-net. We on the other hand present a direct correspondence between a simple multigrid solver and a U-net.

Organisation of the Paper. In Section 2, we translate different numerical approximations for higher order diffusion into CNNs and analyse the resulting architectures. Covering multi-resolution approaches, we show that a multigrid solver can be cast into a U-net form in Section 3. Finally, we present our conclusions and an outlook on future work in Section 4.

2   Networks from Algorithms for Evolution Equations

In this section, we start with generalised diffusion filters in 1D, and we translate three numerical algorithms for them into neural network architectures. This gives novel insights into the value of skip connections, stable network design, and the potential of nonmonotone activation functions.

2.1   Generalised Nonlinear Diffusion

We consider a generalised higher order nonlinear diffusion model in 1D. It creates filtered signals $u(x,t) : (a,b) \times [0,\infty) \to \mathbb{R}$ from an initial signal $f(x)$ on a domain $(a,b) \subset \mathbb{R}$ according to the PDE

$$\partial_t u = -\mathcal{D}^* \big(g\big(|\mathcal{D}u|^2\big) \, \mathcal{D}u \big) \tag{1}$$

which is the gradient flow that minimises the energy $E(u) = \int_a^b \Psi(|\mathcal{D}u|^2) \, dx$ with $g = \Psi'$. We use a general differential operator $\mathcal{D} = \sum_{m=0}^M \alpha_m \partial_x^m$ and its adjoint version $\mathcal{D}^* = \sum_{m=0}^M (-1)^m \alpha_m \partial_x^m$, both consisting of weighted derivatives of up to order M. Thus, the corresponding PDE is of order $2M$. The evolution is initialised at time $t = 0$ by $u(x,0) = f(x)$, and we impose reflecting boundary conditions at $x = a$ and $x = b$. Equation (1) creates gradually simplified versions of f. The scalar *diffusivity* function $g(s^2)$ controls the amount of smoothing depending on the local structure of the evolving signal. We consider diffusivities that are smooth, nonnegative, nonincreasing, and bounded from above.

Depending on the operator $\mathcal{D}$ and the choice of the diffusivity, the evolution describes different models. For $\mathcal{D} = \partial_x$, one obtains a 1D version of the nonlinear diffusion filter of Perona and Malik [19]. For this model the exponential diffusivity $g(s^2) = \exp(-s^2/(2\lambda^2))$ inhibits smoothing near discontinuities where $|\partial_x u|$ exceeds a contrast parameter λ. This allows discontinuity-preserving smoothing. A higher order choice of $\mathcal{D} = \partial_x^2$ yields a 1D version of the fourth order PDE of You and Kaveh [26].

2.2 Residual Networks

Residual networks [11] are a popular CNN architecture as they are easy to train, even for a high number of network layers. They consist of chained residual blocks. A residual block is made up of two convolutional layers with biases and nonlinear activation functions after each layer. Each block computes a discrete output $\boldsymbol{u}$ from an input $\boldsymbol{f}$ by

$$\boldsymbol{u} = \sigma_2(\boldsymbol{f} + \boldsymbol{W}_2\,\sigma_1(\boldsymbol{W}_1\boldsymbol{f} + \boldsymbol{b}_1) + \boldsymbol{b}_2)\,, \tag{2}$$

with discrete convolution matrices $\boldsymbol{W}_1, \boldsymbol{W}_2$, activation functions σ_1, σ_2 and bias vectors $\boldsymbol{b}_1, \boldsymbol{b}_2$. The main difference to feed-forward CNNs lies in the skip connection which adds the original input signal $\boldsymbol{f}$ to the result of the inner activation function σ_1. This facilitates training of very deep networks.

2.3 Expressing Explicit Schemes as Residual Networks

In the following, we derive a direct correspondence between an explicit scheme for the generalised diffusion equation (1) and a ResNet. With the help of the *flux function* $\Phi(s) = g(s^2)\,s$, we rewrite (1) as

$$\partial_t u = -\mathcal{D}^*(\Phi(\mathcal{D}u))\,. \tag{3}$$

We now discretise this equation with an explicit finite difference scheme. To obtain discrete vectors $\boldsymbol{u}, \boldsymbol{f} \in \mathbb{R}^N$, we sample the continuous functions u, f with distance h. We employ a forward difference with time step size τ for the time derivative. Moreover, we represent a discretisation of the operator $\mathcal{D}$ by a convolution matrix $\boldsymbol{K}$. Thus, the adjoint operator $\mathcal{D}^*$ is represented by $\boldsymbol{K}^\top$.

Starting with an initial signal $\boldsymbol{u}^0 = \boldsymbol{f}$, the evolving signal $\boldsymbol{u}^{k+1}$ at time step $k+1$ arises from the previous one by

$$\boldsymbol{u}^{k+1} = \boldsymbol{u}^k - \tau\boldsymbol{K}^\top\boldsymbol{\Phi}\big(\boldsymbol{K}\boldsymbol{u}^k\big)\,. \tag{4}$$

In this notation, the connection between an explicit diffusion step and a ResNet block becomes apparent:

Theorem 1 (Diffusion-inspired ResNets). *A higher order diffusion step* (4) *is equivalent to a residual block* (2) *if*

$$\sigma_1 = \tau\,\boldsymbol{\Phi}, \quad \sigma_2 = \mathrm{Id}, \quad \boldsymbol{W}_1 = \boldsymbol{K}, \quad \boldsymbol{W}_2 = -\boldsymbol{K}^\top, \tag{5}$$

and the bias vectors $\boldsymbol{b}_1$, $\boldsymbol{b}_2$ *are set to* $\boldsymbol{0}$.

Interestingly, the inner activation function σ_1 corresponds to a scaled version of the flux function $\boldsymbol{\Phi}$. The effect of the skip connection in the residual block also becomes clear now: It is the central component to realise a time discretisation. We call a ResNet block of this form a *diffusion block*. It is visualised in Figure 1(a). Graph nodes contain the current state of the signal, while edges describe operations which are applied to proceed from one node to the next.

We observe that the convolution matrices satisfy $\boldsymbol{W}_2 = -\boldsymbol{W}_1^\top$. This is a direct consequence of the gradient flow structure of the diffusion process. In the following, we prove stability and well-posedness for this specific form of ResNets.
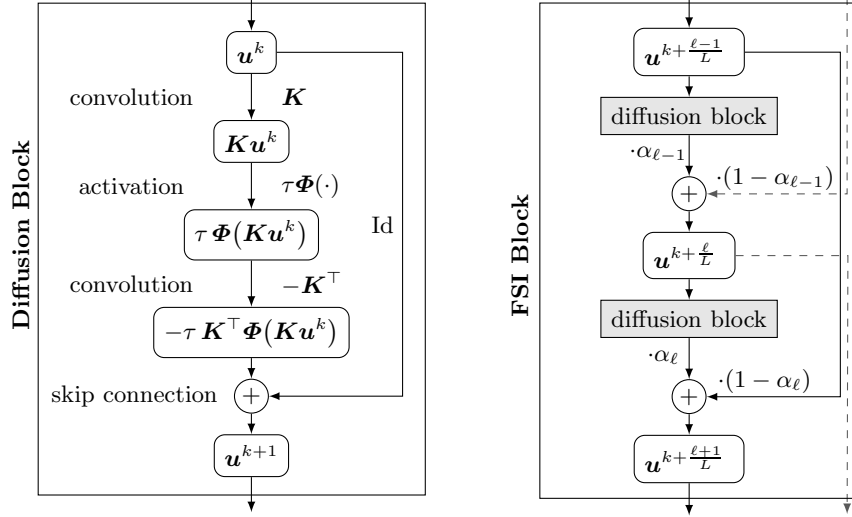
Fig. 1: (a) Left: Diffusion block for an explicit diffusion step (4) with flux function $\boldsymbol{\Phi}$, time step size τ, and a discrete derivative operator $\boldsymbol{K}$. (b) Right: FSI block.

2.4   Criteria for Well-posed and Stable Residual Networks

Now we are able to transfer stability [5] and well-posedness [24] results for diffusion to a residual network consisting of diffusion blocks. We show Euclidean stability, which states that the Euclidean norm of the signal is nonincreasing in each iteration, i.e. $||\boldsymbol{u}^{k+1}||_2 \leq ||\boldsymbol{u}^k||_2$. Well-posedness guarantees that the network output is a continuous function of the input data.

Theorem 2 (Euclidean Stability of ResNets with Diffusion Blocks).
Consider a residual network chaining any number of diffusion blocks (4) with convolutions represented by a convolution matrix $\boldsymbol{K}$ and activation function $\tau\boldsymbol{\Phi}$. Moreover, assume that the activation function arises from a diffusion flux function $\Phi(s) = g(s^2)\,s$ with finite Lipschitz constant L. Then the residual network is well-posed and stable in the Euclidean norm if $\tau \leq 2\left(L||\boldsymbol{K}||_2^2\right)^{-1}$. Here, $||\cdot||_2$ denotes the spectral norm which is induced by the Euclidean norm.

Proof. We first notice that since $\Phi(s) = g(s^2)\,s$, applying the flux function leads to a rescaling with a diagonal matrix $\boldsymbol{G}(\boldsymbol{u}^k)$ with $g((\boldsymbol{K}\boldsymbol{u}^k)_i^2)$ as i-th diagonal element. Therefore, we can write (4) as

$$\boldsymbol{u}^{k+1} = \left(\boldsymbol{I} - \tau\boldsymbol{K}^\top\boldsymbol{G}(\boldsymbol{u}^k)\boldsymbol{K}\right)\boldsymbol{u}^k. \tag{6}$$

At this point, well-posedness follows directly from the continuity of the operator $\boldsymbol{I} - \tau\boldsymbol{K}^\top\boldsymbol{G}(\boldsymbol{u}^k)\boldsymbol{K}$, as the diffusivity g is assumed to be smooth [24].

We now show that the time step size restriction guarantees that the eigenvalues of the operator always lie in the interval $[-1, 1]$. As the spectral norm

is sub-multiplicative, we can estimate the eigenvalues of $\boldsymbol{K}^\top \boldsymbol{G}(\boldsymbol{u}^k)\boldsymbol{K}$ for each matrix separately. Since g is nonnegative, the diagonal matrix $\boldsymbol{G}$ is positive semi-definite. The maximal eigenvalue of $\boldsymbol{G}$ is the given by the supremum of g. As g is non-increasing and bounded, this value is bounded by the Lipschitz constant L of $\varPhi$. Thus, the eigenvalues of $\boldsymbol{K}^\top \boldsymbol{G}(\boldsymbol{u}^k)\boldsymbol{K}$ lie in the interval $[0, \tau L ||\boldsymbol{K}||_2^2]$. Consequently, the operator $\boldsymbol{I} - \tau \boldsymbol{K}^\top \boldsymbol{G}(\boldsymbol{u}^k)\boldsymbol{K}$ has eigenvalues in $[1 - \tau L ||\boldsymbol{K}||_2^2, 1]$, and the condition $1 - \tau L ||\boldsymbol{K}||_2^2 \geq -1$ leads to the bound $\tau \leq 2 \left(L ||\boldsymbol{K}||_2^2\right)^{-1}$. $\quad\square$

How General is this Result? Theorem 2 is of fairly general nature and applies to a broad class of ResNets. The fact that $\boldsymbol{K}$ represents a discrete differential operator is no restriction on the convolution, since any convolution kernel can be seen as a discretisation of a suitable differential operator $\mathcal{D} = \sum_{m=0}^{M} \alpha_m \partial_x^m$.

Interestingly, our proof does not require the matrix $\boldsymbol{K}$ to have a convolution structure: It can be any arbitrary matrix. This even includes neural networks beyond CNNs, since the weights within a layer may differ from node to node.

> **The key requirement for network stability is the transposed convolution structure $W_2 = -W_1^T$.**

While this requirement is not fulfilled by the original ResNet [11], several works employ the transposed structure [3,22,27] as it is justified from a PDE perspective, requires less parameters, and provides stability guarantees.

In contrast to Ruthotto and Haber [22], our stability result does not require activation functions to be monotone. Let us now see that widely used diffusivities naturally lead to nonmonotone activation functions.

2.5   Nonmonotone Activation Functions

The connection between diffusivity $g(s^2)$ and activation function $\sigma(s) = \tau \varPhi(s)$ with the diffusion flux $\varPhi(s) = g(s^2)s$ revitalises an old idea of neural network design [4,15]. As an example, we translate the exponential Perona–Malik diffusivity $g(s^2) = \exp\left(-\frac{s^2}{2\lambda^2}\right)$ into its corresponding activation $\sigma(s) = \tau s \exp\left(-\frac{s^2}{2\lambda^2}\right)$. Interestingly, this activation function is *antisymmetric* and *nonmonotone.*

Antisymmetry is very natural in the diffusion case with $\mathcal{D} = \sum_{m=1}^{M} \alpha_m \partial_x^m$, where the argument of the flux function consists of signal derivatives. It reflects the invariance axiom that signal negation and filtering are commutative. Nonmonotone flux functions were considered somewhat problematic for continuous diffusion PDEs. However, it has been shown that their discretisations are well-posed [25], in spite of the fact that they may act contrast enhancing.

The concept of a nonmonotone activation function is unusual in the CNN world. Although there have been a few early proposals in the neural network literature arguing in favour of nonmonotone activations [4,15], they are rarely used in modern CNNs. In practice, CNNs often fix the activation to simple functions such as the rectified linear unit (ReLU). From a PDE perspective, this appears restrictive. The diffusion interpretation suggests that activation

functions should be learned in the same manner as convolution weights and biases. In practice, this hardly happens apart from a few notable exceptions such as [3,7,17]. As nonmonotone flux functions outperform monotone ones in the diffusion setting, it appears promising to incorporate them into CNNs. For more examples of diffusion-inspired activation functions, we refer to [1].

2.6   FSI Schemes and Additional Skip Connections

In the following, we show that an acceleration strategy of the explicit scheme induces a natural modification for the skip connections of the corresponding ResNet architecture. To speed up explicit schemes, Hafner et al. [9] proposed *fast semi-iterative* (FSI) schemes. They perform a cycle of extrapolated explicit steps. For our diffusion scheme (4), an FSI acceleration with cycle length L reads

$$\boldsymbol{u}^{k+\frac{\ell+1}{L}} = \alpha_\ell \left(\boldsymbol{I} - \tau \boldsymbol{K}^\top \boldsymbol{\Phi}\left(\boldsymbol{K}\boldsymbol{u}^{k+\frac{\ell}{L}}\right)\right) + (1 - \alpha_\ell)\,\boldsymbol{u}^{k+\frac{\ell-1}{L}} \tag{7}$$

with $\ell = 0, \ldots, L-1$ and extrapolation weights $\alpha_\ell := (4\ell + 2)/(2\ell + 3)$. One formally initialises with $\boldsymbol{u}^{k-\frac{1}{L}} := \boldsymbol{u}^k$. This cycle realises a super time step of size $\frac{L(L+1)}{3}\tau$. Thus, with one cycle involving L explicit steps, one reaches a super step size of $\mathcal{O}(L^2)$ rather than $\mathcal{O}(L)$. This explains its remarkable efficiency [9].

We see that FSI extrapolates the diffusion result at time step $k + \frac{\ell}{L}$ with the previous time step $k + \frac{\ell-1}{L}$ and the weight α_ℓ. This can be realised with a small change in the original diffusion block from Figure 1(a) by adding an additional skip connection. The two skip connections are weighted by α_ℓ and $(1 - \alpha_\ell)$, respectively. This gives the architecture in Figure 1(b).

We observe a different benefit of skip connections: Additional and more general skip connections constitute a whole class of acceleration strategies, which is in line with observations in the CNN literature; see e.g. [13,14].

2.7   Implicit Schemes and Recurrent Neural Networks

So far, we have connected variants of explicit schemes to ResNets. However, implicit discretisations are another important class of solvers. We now show that such a discretisation of our diffusion equation leads to a recurrent neural network (RNN). RNNs are classical neural network architectures; see e.g. [12]. The fully implicit discretisation of (1) is given by

$$\boldsymbol{u}^{k+1} = \boldsymbol{u}^k - \tau \boldsymbol{K}^\top \boldsymbol{\Phi}\left(\boldsymbol{K}\boldsymbol{u}^{k+1}\right). \tag{8}$$

We solve the resulting nonlinear system of equations by L fixed point iterations:

$$\boldsymbol{u}^{k+\frac{\ell+1}{L}} = \boldsymbol{u}^k - \tau \boldsymbol{K}^\top \boldsymbol{\Phi}\left(\boldsymbol{K}\boldsymbol{u}^{k+\frac{\ell}{L}}\right), \tag{9}$$

where $\ell = 0, \ldots, L-1$, and where we assume that τ is sufficiently small to yield a contraction mapping. For $L = 1$, we obtain the explicit scheme (4) with its ResNet interpretation. For larger L, however, different skip connections arise.

They connect the layer at time step k with all subsequent layers at steps $k + \frac{\ell}{L}$ with $\ell = 0, \ldots, L-1$. This feedback can be seen as an RNN architecture.

In the context of variational models, Chen and Pock [3] have obtained a similar architecture. However, they explicitly supplement the diffusion process with an additional reaction term which results from the data term of the energy. Our feedback term is a pure numerical phenomenon of the fixed point solver.

We see that skip connections can implement a number of successful numerical concepts: forward difference approximations of the time derivative in explicit schemes, extrapolation steps to accelerate them e.g. via FSI, and recurrent connections within fixed point solvers for implicit schemes.

3   Multigrid Solvers and U-nets

Multigrid methods [2] are very efficient numerical strategies for solving PDE-based problems. Neural networks, on the other hand, have benefitted from multiscale ideas as well, as can be seen e.g. from the high popularity of U-nets [20]. In this section we shed some light on their structural connections. For simplicity we restrict ourselves to a linear multigrid setting with two levels.
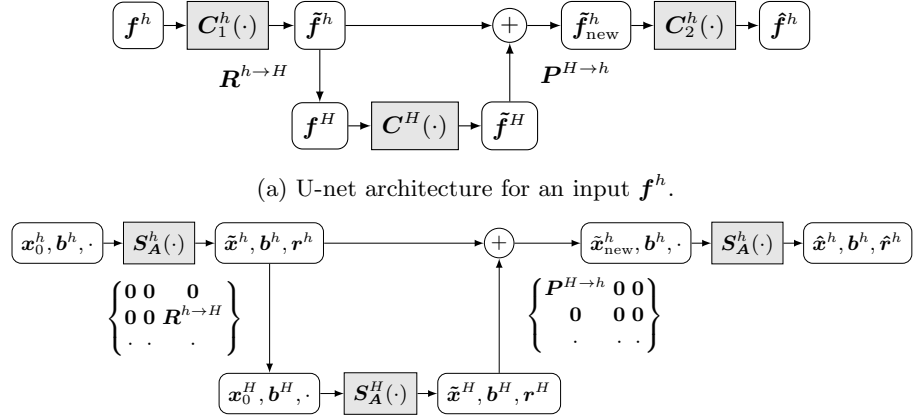
3.1   U-net Architectures

The U-net [20] has proven useful in applications such as segmentation [20] or pose estimation [16], where features on multiple scales need to be extracted

As its name suggests, the U-net has a symmetric shape: On the left half of the architecture, convolutions extract features while repeated downsampling operators reduce the resolution. On the right half, features are successively upsampled, combined and convolved, starting with the coarsest resolution. The original U-net [20] combines features by concatenation, while other works such as [16] use addition. In the following, we focus on the latter design choice.

For our purposes, it is sufficient to consider a U-net with only two resolutions and a constant number of channels. We use superscripts h and H to denote computations on the fine and coarse grid, respectively. The following six steps capture the essential structure of such a U-net:

1. One applies a number of CNN layers to the input $\boldsymbol{f}^h$, yielding a modified signal $\tilde{\boldsymbol{f}}^h$. We denote this general operation by a function $\boldsymbol{C}_1^h(\cdot)$.
2. To provide a coarse input $\boldsymbol{f}^H = \boldsymbol{R}^{h \to H} \tilde{\boldsymbol{f}}^h$ to the next level, a restriction operator $\boldsymbol{R}^{h \to H}$ brings the modified signal $\tilde{\boldsymbol{f}}^h$ to a coarse resolution H. For example, the restriction can consist of an averaging or max-pooling.
3. On the coarse grid, the downsampled signal $\boldsymbol{f}^H$ is again modified by a series of layers to obtain $\tilde{\boldsymbol{f}}^H = \boldsymbol{C}^H(\boldsymbol{f}^H)$.
4. One upsamples the coarse result $\tilde{\boldsymbol{f}}^H$ with a prolongation operator $\boldsymbol{P}^{H \to h}$.
5. On the fine grid, one adds the modified fine grid signal $\tilde{\boldsymbol{f}}^h$ and the upsampled one $\boldsymbol{P}^{H \to h} \boldsymbol{f}^H$ and obtains $\tilde{\boldsymbol{f}}_{\text{new}}^h$.
6. Lastly, applying more layers $\boldsymbol{C}_2^h(\cdot)$ yields the final solution $\hat{\boldsymbol{f}} = \boldsymbol{C}_2^h(\tilde{\boldsymbol{f}}_{\text{new}}^h)$.

Figure 2(a) visualises this architecture. In the following, we express a multigrid V-cycle in this form by utilising multiple network channels.

(a) U-net architecture for an input $\boldsymbol{f}^h$.

(b) Two-level V-Cycle in the form of a U-net utilising three-channel signals containing the iteration variable $\boldsymbol{x}$, a right hand side $\boldsymbol{b}$, and the residual $\boldsymbol{r}$.

Fig. 2: Architectures for a general U-net and a multigrid V-cycle.

3.2 Expressing a Multigrid V-cycle within a U-net

Multigrid methods [2] allow for the efficient solution of equation systems that result from the numerical approximation of PDEs. For simplicity we consider a linear system of equations given by $\boldsymbol{Ax} = \boldsymbol{b}$. For classical iterative solvers such as the Jacobi or the Gauss–Seidel method, one observes that low-frequent error components are attenuated only very slowly. Hence, their convergence is slow. Multigrid methods transfer the low-frequent error components to a coarser scale, where the iterative solvers work more efficiently. The coarse scale solution is then used to correct the fine scale approximation.

To connect multigrid ideas to U-nets, we consider a V-cycle on two levels with grid sizes h and H for the fine and coarse grid. For our U-net, we use three channels. They contain the iteration variable $\boldsymbol{x}$ of the solver, the right hand side $\boldsymbol{b}$ of the equation system, and the current residual $\boldsymbol{r}$. Even though we do not always need all channels, we keep the channel number constant for simplicity. A two-level V-cycle solves the linear system by repeating the following steps:

1. The inputs are a fine grid initialisation $\boldsymbol{x}_0^h = \boldsymbol{0}$ and the given right hand side $\boldsymbol{b}^h$. The residual at this point is ignored, as it is not relevant to the solver input. We assume that we are given a solver $\boldsymbol{S}_{\boldsymbol{A}}^h(\cdot)$ for the operator $\boldsymbol{A}^h$. It produces a three-channel signal containing an approximate solution $\tilde{\boldsymbol{x}}^h$, the right hand side $\boldsymbol{b}^h$, and a residual $\boldsymbol{r}^h = \boldsymbol{b}^h - \boldsymbol{A}^h\tilde{\boldsymbol{x}}^h$.
2. While the true error $\boldsymbol{e}^h$ of the approximation is unknown, the residual $\boldsymbol{r}^h$ can be computed. This leads to the residual equation $\boldsymbol{A}^h\boldsymbol{e}^h = \boldsymbol{r}^h$ which can be solved efficiently on a coarser grid. To this end, one uses a restriction operator $\boldsymbol{R}^{h\to H}$. As the downsampling is now explicitly concerned with three channels, the corresponding operator in the CNN is a 3×3 block matrix. The

coarse initialisation $x_0^H = 0$ does not require any information from the fine scale. Crucially, the new right hand side b^H is the downsampled fine residual, i.e. $b^H = R^{h \to H} r^h$. Lastly, an input residual is not required for the coarse solver. Thus, one obtains the coarse grid residual equation $A^H x^H = b^H$.

3. The coarse grid solver $S_A^H(\cdot)$ now solves the residual equation. It outputs a coarse approximation $\tilde{x}^H$ to the residual error, the right hand side b^H, and a new coarse residual r^H. The latter two would be required if one wants to add another level to the cycle.

4. In the upsampling step, we prepare the coarse scale outputs for the following addition. Similar to the downsampling, we upsample only the coarse error approximation $\tilde{x}^H$ by a prolongation operator $P^{H \to h}$. The coarse right hand side b^H is set to 0 as to not interfere with the fine right hand side.

5. On the fine grid, one adds the three signal channels. The initial fine grid approximation is updated with the upsampled error on the coarse grid by $\tilde{x}_{\text{new}}^h := \tilde{x}^h + P^{H \to h} \tilde{x}^H$. As we have applied the prolongation only to the coarse solution, the fine grid right hand side b^h is propagated.

6. Another instance of the fine grid solver $S_A^h(\cdot)$ takes the corrected solution x_{new}^h and the original right hand side b^h, yielding a new approximation $\hat{x}^h$.

We visualise this architecture in Figure 2(b). Restriction and prolongation operators are applied only to certain channels of the solver output instead of all channels. In the downsampling phase, the restriction is applied to the residual, while in the upsampling phase, it is applied to the approximated error. This enables the coarse solver to work on the residual equation instead of only a coarse version of the original equation, which is the crucial idea of multigrid methods. The architecture utilises yet another form of skip connection: The fine scale approximation is corrected by adding an upsampled error approximation.

Our two-level setting can be generalised to more levels. Deeper V-cycles are constructed by stacking the two-level V-cycle recursively, and so-called W-cycles are built by concatenating two V-cycles. On the CNN side, this leads to U-nets with more levels, as well as concatenations thereof. This idea is also used in practice: Successful U-nets work on multiple resolutions [20], and so-called stacked hourglass models [16] arise by concatenating multiple V-cycle architectures. It shows that multigrid architectures share essential structural properties with U-nets.

4   Conclusions

Our paper is based on the philosophy of regarding a trained neural network as a numerical algorithm. To substantiate this claim, we have translated a number of efficient numerical algorithms for PDEs into popular building blocks for network architectures. Apart from a few notable exceptions such as [14], this strategy has rarely been pursued in its full consequence. We have shown that valuable structural insights can be gained from such a direct translation, and we have derived systematic design principles for well-founded network components.

More specifically, we have shown the value of skip connections from three different numerical perspectives: as time discretisations in explicit schemes, as extrapolation terms to increase their efficiency, and as recurrent connections in implicit schemes with fixed point structure. By connecting multigrid methods to U-nets, we provide a basis for explaining for their remarkable efficiency. Numerical schemes for generalised diffusion processes suggest that nonmonotone activation functions are permissible and can be advantageous. Last but not least, we have seen that a ResNet block with a transposed structure of both convolution layers can guarantee Euclidean stability in a simple and elegant way.

Our contributions can serve as a blueprint for translating a larger class of successful numerical concepts for PDEs to CNNs. This is part of our ongoing work. It is our hope that this will lead to a closer connection of both worlds and to hybrid methods that unite the stability and efficiency of modern numerical algorithms with the performance of neural networks.

References

1. Alt, T., Weickert, J., Peter, P.: Translating diffusion, wavelets, and regularisation into residual networks. arXiv:2002.02753v3 [cs.LG] (Jun 2020)
2. Briggs, W.L., Henson, V.E., McCormick, S.F.: A Multigrid Tutorial. SIAM, Philadelphia, second edn. (2000)
3. Chen, Y., Pock, T.: Trainable nonlinear reaction diffusion: A flexible framework for fast and effective image restoration. IEEE Transactions on Pattern Analysis and Machine Intelligence **39**(6), 1256–1272 (Aug 2016)
4. De Felice, P., Marangi, C., Nardulli, G., Pasquariello, G., Tedesco, L.: Dynamics of neural networks with non-monotone activation function. Network: Computation in Neural Systems **4**(1), 1–9 (1993)
5. Didas, S., Weickert, J., Burgeth, B.: Properties of higher order nonlinear diffusion filtering. Journal of Mathematical Imaging and Vision **35**, 208–226 (Nov 2009)
6. Eliasof, M., Ephrath, J., Ruthotto, L., Treister, E.: Multigrid-in-Channels neural network architectures. arXiv:2011.09128v2 [cs.CV] (Nov 2020)
7. Goodfellow, I., Warde-Farley, D., Mirza, M., Courville, A., Bengio, Y.: Maxout networks. In: Dasgupta, S., McAllester, D. (eds.) Proc. 30th International Conference on Machine Learning. Proceedings of Machine Learning Research, vol. 28, pp. 1319–1327. Atlanta, GA (Jun 2013)
8. Greenfeld, D., Galun, M., Kimmel, R., Yavneh, I., Basri, R.: Learning to optimize multigrid PDE solvers. In: Chaudhuri, K., Salakhutdinov, R. (eds.) Proc. 36th International Conference on Machine Learning. Proceedings of Machine Learning Research, vol. 97, pp. 2415–2423. Long Beach, CA (Jun 2019)
9. Hafner, D., Ochs, P., Weickert, J., Reißel, M., Grewenig, S.: FSI schemes: Fast semi-iterative solvers for PDEs and optimisation methods. In: Rosenhahn, B., Andres, B. (eds.) Pattern Recognition, Lecture Notes in Computer Science, vol. 9796, pp. 91–102. Springer, Cham (2016)
10. He, J., Xu, J.: MgNet: A unified framework of multigrid and convolutional neural network. Science China Mathematics **62**, 1331–1354 (May 2019)

11. He, K., Zhang, X., Ren, S., Sun, J.: Deep residual learning for image recognition. In: Proc. 2016 IEEE Conference on Computer Vision and Pattern Recognition. pp. 770–778. IEEE Computer Society Press, Las Vegas, NV (Jun 2016)
12. Hopfield, J.J.: Neural networks and physical systems with emergent collective computational abilities. Proceedings of the National Academy of Sciences **79**(8), 2554–2558 (Apr 1982)
13. Huang, G., Liu, Z., van der Maaten, L., Weinberger, K.Q.: Densely connected convolutional networks. In: Proc. 2017 IEEE Conference on Computer Vision and Pattern Recognition. pp. 4700–4708. IEEE Computer Society Press, Honolulu, HI (Jul 2017)
14. Lu, Y., Zhong, A., Li, Q., Dong, B.: Beyond finite layer neural networks: Bridging deep architectures and numerical differential equations. In: Dy, J., Krause, A. (eds.) Proc. 35th International Conference on Machine Learning. Proceedings of Machine Learning Research, vol. 80, pp. 3276–3285. Stockholm, Sweden (Jul 2018)
15. Meilijson, I., Ruppin, E.: Optimal signalling in attractor neural networks. In: Tesauro, G., Touretzky, D., Leen, T. (eds.) Proc. 7th Annual Conference on Neural Information Processing Systems. Advances in Neural Information Processing Systems, vol. 7, pp. 485–492. Denver, CO (Dec 1994)
16. Newell, A., Yang, K., Deng, J.: Stacked hourglass networks for human pose estimation. In: Leibe, B., Matas, J., Sebe, N., Welling, M. (eds.) Computer Vision – ECCV 2016, Lecture Notes in Computer Science, vol. 9912, pp. 483–499. Springer, Cham (2016)
17. Ochs, P., Meinhardt, T., Leal-Taixe, L., Möller, M.: Lifting layers: Analysis and applications. In: Ferrari, V., Herbert, M., Sminchisescu, C., Weiss, Y. (eds.) Computer Vision – ECCV 2018, Lecture Notes in Computer Science, vol. 11205, pp. 53–68. Springer, Cham (2018)
18. Ouala, S., Pascual, A., Fablet, R.: Residual integration neural network. In: Proc. 2019 IEEE International Conference on Acoustics, Speech and Signal Processing. pp. 3622–3626. IEEE Computer Society Press, Brighton, UK (May 2019)
19. Perona, P., Malik, J.: Scale space and edge detection using anisotropic diffusion. IEEE Transactions on Pattern Analysis and Machine Intelligence **12**, 629–639 (Jul 1990)
20. Ronneberger, O., Fischer, P., Brox, T.: U-net: Convolutional networks for biomedical image segmentation. In: Navab, N., Hornegger, J., Wells, W., Frangi, A. (eds.) Medical Image Computing and Computer-Assisted Intervention – MICCAI 2015, Lecture Notes in Computer Science, vol. 9351, pp. 234–241. Springer, Cham (2015)
21. Rousseau, F., Drumetz, L., Fablet, R.: Residual networks as flows of diffeomorphisms. Journal of Mathematical Imaging and Vision **62**, 365–375 (Apr 2020)
22. Ruthotto, L., Haber, E.: Deep neural networks motivated by partial differential equations. Journal of Mathematical Imaging and Vision **62**, 352–364 (Apr 2020)
23. Smets, B., Portegies, J., Bekkers, E., Duits, R.: PDE-based group equivariant convolutional neural networks. arXiv:2001.09046v2 [cs.LG] (Mar 2020)
24. Weickert, J.: Anisotropic Diffusion in Image Processing. Teubner, Stuttgart (1998)
25. Weickert, J., Benhamouda, B.: A semidiscrete nonlinear scale-space theory and its relation to the Perona–Malik paradox. In: Solina, F., Kropatsch, W.G., Klette, R., Bajcsy, R. (eds.) Advances in Computer Vision, pp. 1–10. Springer, Wien (1997)
26. You, Y.L., Kaveh, M.: Fourth-order partial differential equations for noise removal. IEEE Transactions on Image Processing **9**(10), 1723–1730 (Oct 2000)
27. Zhang, L., Schaeffer, H.: Forward stability of ResNet and its variants. Journal of Mathematical Imaging and Vision **62**, 328–351 (Apr 2020)